Presented at the 38th European PV Solar Energy Conference and Exhibition, 6-10 September 2021

EFFECTS OF INHOMOGENEOUS SNOW LOAD ON THE MECHANICS OF A PV MODULE

Pascal Romer[1], Andreas J. Beinert[1]
[1]Fraunhofer Institute for Solar Energy Systems ISE, Heidenhofstraße 2, 79110 Freiburg, Germany.
Corresponding author: Pascal Romer | Phone: +49 (0)761 4588 5044 | E-mail: Pascal.Romer@ise.fraunhofer.de

ABSTRACT: The phenomenon that snow sliding down a tilted PV-module can cause an inhomogeneous load is well known. However, just in 2020 a standard for this load scenario was established with the IEC 62938. This paper compares the difference between a homogeneous and such an inhomogeneous load distribution. Additionally, the influence of different temperatures on this new standard is analyzed. Compared to a homogeneous load distribution the first principal stress is lower for an inhomogeneous distribution. Moreover, it is shown that temperature has a large influence on the stress during mechanical loading. For TPO there is a specific temperature at which both the first principal stress and the probability of cell fracture reach a maximal value.

Keywords: Finite element modelling, FEM simulations, inhomogeneous snow load, photovoltaic module, stress, thermomechanics, mechanical load, virtual prototyping, coefficient of thermal expansion, material characterization.

1 INTRODUCTION

According to the IEC 61215 [1] a homogeneous mechanical load of at least 2400 Pa at 25 °C is one criteria to pass the certification. However, in the field load is often distributed inhomogeneously over the module and occurs mainly at temperatures different from 25 °C. Therefore the IEC 62938 [2] proposes a non-uniform snow load test for photovoltaic modules. A lot of papers investigate a homogeneous mechanical load according to IEC 61215 [3–10]. A few others deal with an non-uniform load due to wind [11, 12] and snow [12], but to the present knowledge none of them investigate the load according to IEC 62938. Hence, this work analyzes the effect of such a non-uniform snow load on the mechanics of a photovoltaic module for TPO (thermoplastic polyolefin) as the encapsulant. Furthermore some experimental works [13, 14] already investigated the influence of the temperature on the homogeneous mechanical load. Therefor this influence is analyzed for the inhomogeneous load using FEM simulations (finite element method).

2 METHOD

2.1 Storage modulus measurement

To analyze the effect of the encapsulants thermal properties, the temperature dependent storage modulus of TPO is measured with a DMA Eplexor from Netzsch Gabo. Due to the melting point of TPO, the storage modulus is only measured from -60 °C up to 80 °C and then extrapolated with a constant value for the FEM simulations. The samples are measured with an oscillation frequency of 1 Hz and a temperature ramp of 2 K/min.

2.2 CTE measurement

The coefficient of thermal expansion (CTE) is measured using a DMA242 C from Netzsch. To ensure that only the sample's thermal expansion is analyzed, a reference measurement using copper, with a known CTE, is carried out. Based on this measurement, thermal expansion of the DMA is calculated and can later be subtracted from that of the material measurement. Three measurements are performed, and a linear function is fitted to evaluate the CTE.

2.3 FEM simulation

The used FEM model is based on previous studies with neglected metallization and ribbons [4, 5]. Unlike to the referenced FEM models, due to the inhomogeneous load, the PV module exhibits only one symmetry plane. Therefore, half of a 120 half-cell PV module is simulated. In a first step, the lamination process is simulated by using a single temperature drop from 150 °C down to 25 °C. The residual stress from the lamination is used as an initial stress state for the later simulation of the mechanical load. The mechanical load simulation considers an aluminum frame and is performed at -40 °C, -20 °C, 0 °C as well as at 25 °C. Both, the homogeneous as well as the inhomogeneous load, are simulated with an equivalent load of 2400 Pa and 5400 Pa, respectively. Due to the slanted mounting of most PV modules, the snow load is not evenly distributed over the entire module but tends to slide downwards to the edge of the module. To reproduce this behavior the IEC 62938 works with a surface load S_A covering the lower 2/3 of the module combined with a linear load S_E as depicted in Figure 1.

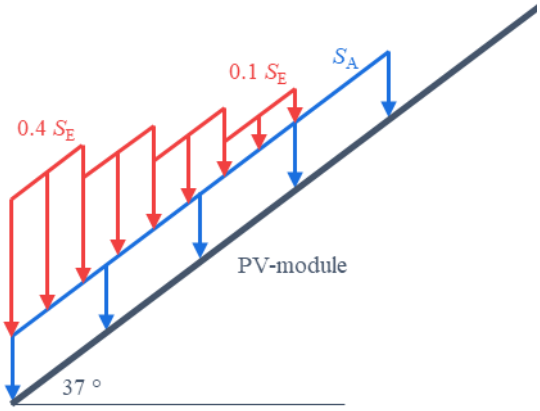

Figure 1: Inhomogeneous load distribution according to IEC 62938 on a PV module, consisting of an uniform surface load (S_A) and a linear load (S_E).

For comparable results between the homogeneous and the inhomogeneous simulations the total load mass must be the same for both cases. To guarantee this for the inhomogeneous simulation, the same load mass, used in the homogeneous case, is distributed unevenly over the pv module according to IEC 62938. The load profiles for the homogeneous as well as the inhomogeneous case that are implemented in the FEM simulation are shown in Figure 2. The material parameters used in the simulation are shown in Table 1.

Table 1: Specifications and material properties of the PV module. *: provided by manufacturer, †: measured.

Layer	Material	Dimension	Density [g/cm³]	Young's modulus [GPa]	Poisson's ratio [-]	CTE [10^{-6}K^{-1}]
Front glass	soda-lime glass	3.2 mm	2.5*	73*	0.24*	9.2*
Encapsulant	TPO	460 µm	0.96 [17]	Table 2†	0.22 [17]	293†
Solar cell	Cz-silicon	166 × 83 × 0.180 mm³	2.329 [17]	Elasticity matrix [17]		T-dep. [15, 16]
Backsheet	TPT	218 µm	2.52 [17]	3.5 [17]	0.29 [17]	50.4 [17]
Frame	aluminum		2.7 [18]	70 [18]	0.33 [18]	23 [18]
Frame-inlay	rubber		0.067*	0.00043*	0.49*	769*

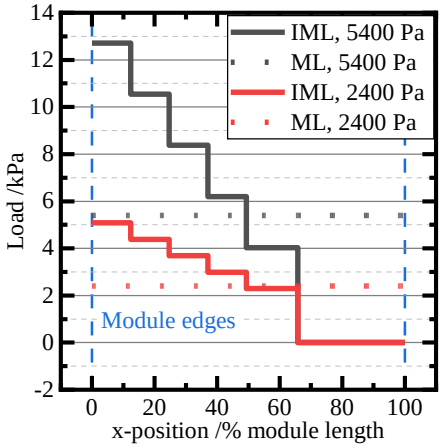

Figure 2: Profiles for the homogeneous as well as the inhomogeneous load distribution, implemented in the FEM simulation.

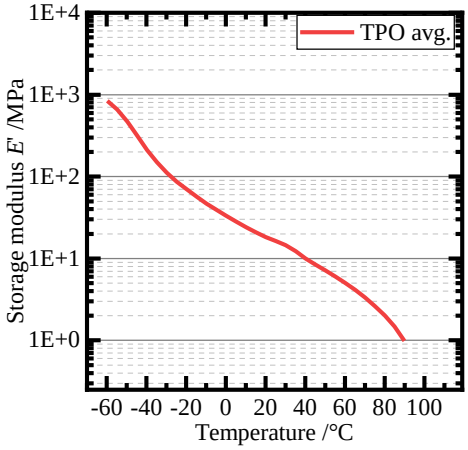

Figure 3: Measured storage modulus for the three different encapsulants EVA, TPO, POE over temperature.

Silicon is a brittle material, which means that solar cells tend to break under tensile stress. This analysis focuses therefore on the first principal stress σ_I (interpreted as tensile stress) during mechanical load. Furthermore, the probability of cell fracture P_fail is calculated using the Weibull distribution [19] considering size effects [20]:

$$P_\mathrm{fail} = 1 - \exp\left(-\sum_\mathrm{i} -A_\mathrm{eff,i}\left(\frac{\sigma_\mathrm{I,max}}{\sigma_\mathrm{0,i}}\right)^{m_\mathrm{i}}\right) \text{ with } A_\mathrm{eff,i} = \int\left(\frac{\sigma_\mathrm{I,i}(x,y)}{\sigma_\mathrm{I,max}}\right)^{m_\mathrm{i}} dA_\mathrm{i} \quad (1)$$

with the effective area A_eff, the maximum first principal stress $\sigma_\mathrm{I,max}$, the Weibull scale factor σ_0 and the Weibull modulus m. Both parameters σ_0 and m are taken from [21]. The effective area A_eff can be interpreted as an equivalent area where the maximum first principal stress $\sigma_\mathrm{I,max}$ occurs. The first principal stress $\sigma_\mathrm{I,i}(x,y)$ at the position (x, y) is integrated over the surface $A_\mathrm{i}(x,y)$. It should be mentioned that the probability of cell fracture is the probability that at least one crack is present in at least one solar cell of the entire module and does not correlate with the expected loss of power.

3 RESULTS

3.1 Storage modulus measurements

The temperature dependent storage modulus is depicted in Figure 3 and can be found in Table 2. TPO shows a glass transition below 0 °C where the storage modulus increases from about 33 MPa at 0 °C to 217 MPa at -40 °C.

3.2 CTE measurements

For the CTE measurement at least three samples are measured, and a linear model is fitted to the data, where the slope is taken as the CTE. Exemplary one sample with the fitted data is shown in Figure 4. The average CTE for TPO is found to be $293 \cdot 10^{-6}\mathrm{K}^{-1}$.

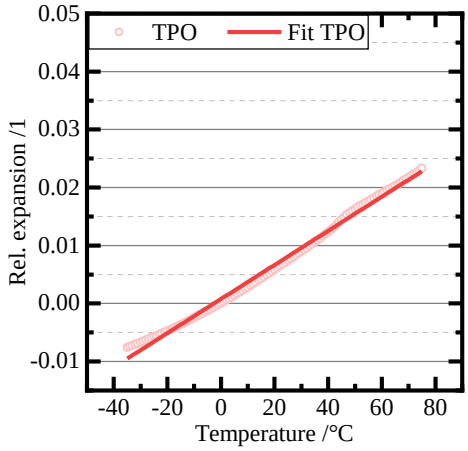

Figure 4: Measured relative expansion for one sample (symbols, light colors) and linear fits to the data (line, dark colors), from which the CTE is taken.

Table 2: Measured storage modulus for the three encapsulants EVA, TPO and POE for temperatures between -55 °C and 90 °C.

Temp / °C	-55	-50	-45	-40	-35	-30	-25	-20	-15	-10	-5	0	5	10	15
E'_{TPO} / MPa	669	479	322	217	153	113	88.0	70.5	57.2	47.2	39.6	33.4	28.4	24.2	20.9
Temp / °C	20	25	30	35	40	45	50	55	60	65	70	75	80	85	90
E'_{TPO} / MPa	18.3	16.4	14.6	12.3	9.98	8.41	7.15	6.06	5.03	4.13	3.34	2.62	2.01	1.48	0.98

3.2 Lamination

The minimum third principal stress $\sigma_{III,min}$ (interpreted as compressive stress) after lamination with TPO as the encapsulant is found to be -93 MPa.

3.3 Mechanical load

In this section the results of the mechanical load simulations will be discussed. First, the homogeneous load test according to IEC 61215 will be compared to the inhomogeneous one out of the IEC 62938, distributed along the module's short side as well as the long side. Second, the temperature dependency of the inhomogeneous load on the resulting first principal stress will be discussed.

Figure 5 exemplary shows the maximal first principal stress as well as the probability of cell fracture for TPO at an equivalent load of 2400 Pa. In all cases the homogeneous and the inhomogeneous ones, the maximal first principal stress is well below the critical value of 177 MPa [21], and accordingly the probability of cell fracture is negligible. Consequently, the following analysis will focus only on the results for an equivalent load of 5400 Pa.

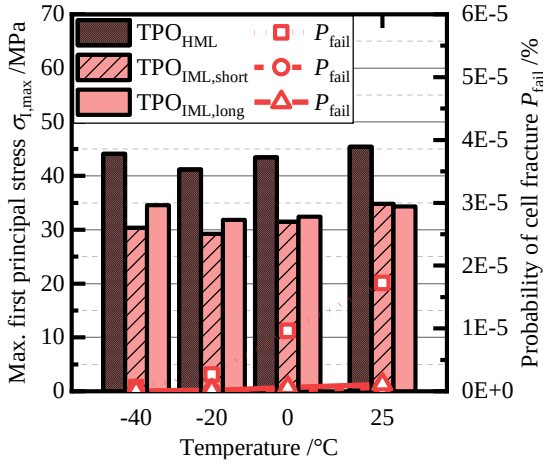

Figure 5: Comparison between the homogeneous and the inhomogeneous load case at 2400 Pa for TPO.

3.3.1 Comparison homogeneous vs. inhomogeneous load

Figure 7 depicts the overall stress distribution at an equivalent load of 5400 Pa and a temperature of 25 °C for a load distributed along the short side (middle) as well as along the module's long side (rigth). Compared to the homogeneous load, the stress distribution of the inhomogeneous load shifts to the loaded PV module side and has a lower overall magnitude on the first principal stress. In Figure 6 the maximal first principal stress as well as the probability of cell fracture is shown for all three load cases. Due to the lower stress during the inhomogeneous loading the cells are less prone to cell fracture.

Even though the homogeneous loading leads to a higher probability of cell fracture, this loading case is well investigated in previous research, therefore the following analysis will focus on the inhomogeneous loading, especially when distributed along the module's long side.

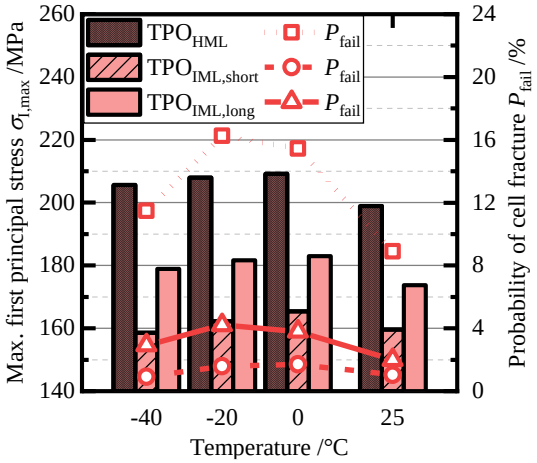

Figure 6: Comparison between the homogeneous and the inhomogeneous load case at 5400 Pa for TPO as a representative for the three encapsulants.

3.3.3 Influence of temperature

In Figure 8 the maximum first principal stress as well as the probability of cell fracture is depicted. Both values depend strongly on the temperature. A maximum in the probability of cell fracture can be seen at -20 °C. To explain this, three different effects must be considered. First, the encapsulant serves as a stress buffer for the solar cells. The colder and therefore the harder the encapsulant the worse the ability to buffer stresses, see Figure 3. Second, the harder the encapsulant the stiffer the whole PV module. Hence, colder temperatures lead to a decrease of the PV module deflection during mechanical loading, shown in Figure 9. Finally, going to colder temperatures, the amplitude of the compressive stress increases due to thermal compression. This can be seen in in the third principal stress in Figure 10, which shows the highest amplitude of the third principal stress in the cells at different temperatures from a FEM simulation without mechanical loading.

The first effect causes an increase of the first principal stress. Opposed to that, the latter two effects lead to a decrease of the first principal stress when going to colder temperatures. Above the glass transition at roughly -20 °C the first effect dominates and below it the latter two become more dominant.

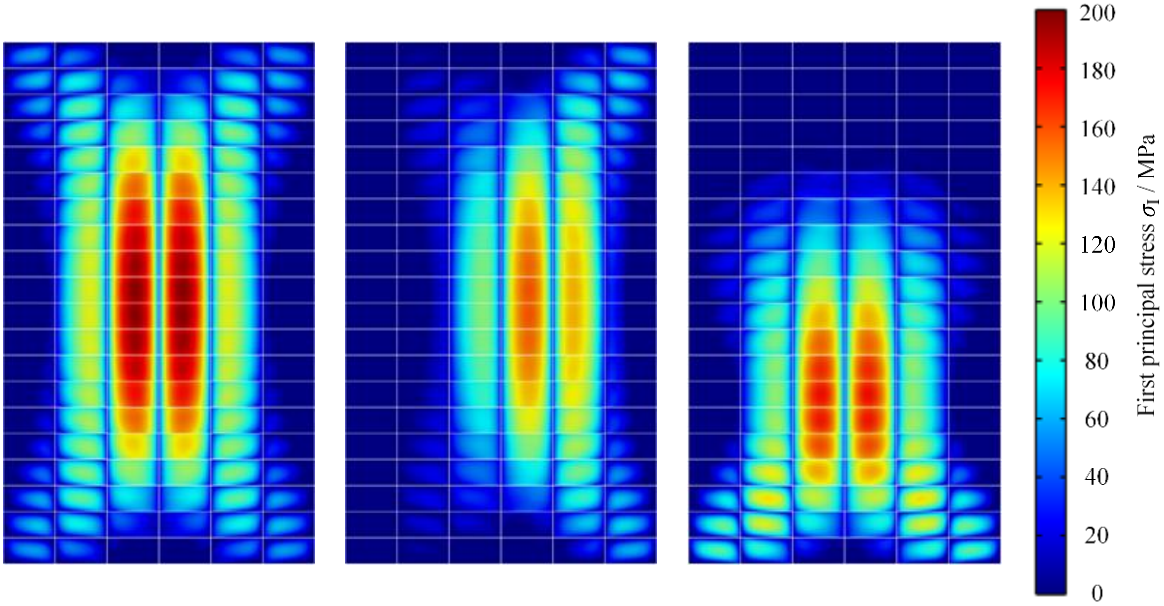

Figure 7: Distribution of the first principal stress σ_I for at an equivalent load of 5400 Pa and 25 °C for a homogeneous load (left) compared to an inhomogeneous loads distributed along the short side of the module (middle) as well as along the module's long side (right).

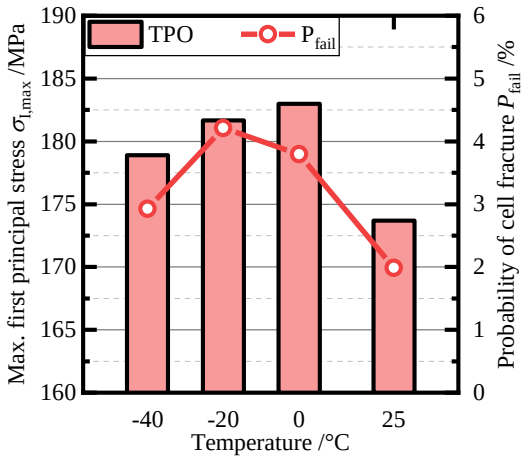

Figure 8: Temperature dependent first principal stress as well as probability of cell fracture for the inhomogeneous distribution with an equivalent load of 5400 Pa

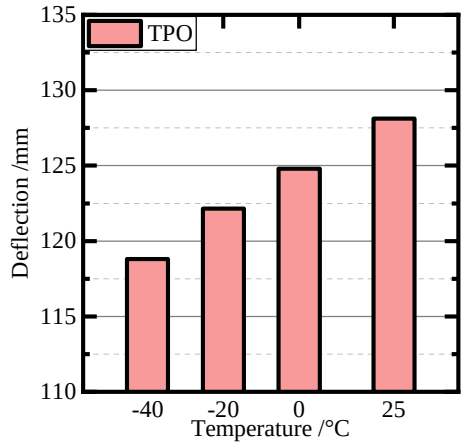

Figure 9: Maximal deflection at an equivalent load of 5400 Pa at different temperatures.

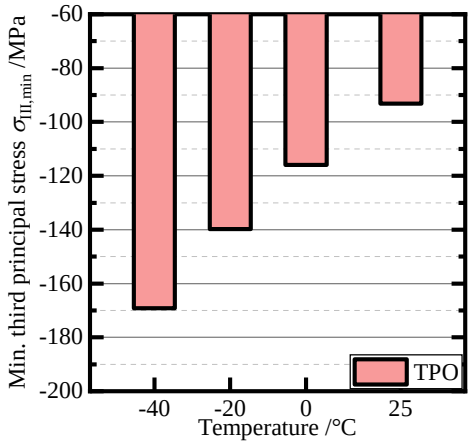

Figure 10: Minimal third principal stress without mechanical loading at different temperatures.

4 CONCLUSIONS

Applying an inhomogeneous load distribution on photovoltaic modules changes the stress distribution in the solar cells. The maximal stress shifts to the lower module edge with higher applied load. Looking at the inhomogeneous load distribution, the maximum first principal stress is significantly lower. Consequently, also the cells are less prone to cell fracture during inhomogeneous loading.

Inhomogeneous loading appears in the field usually not at room temperature, as specified in the IEC 62938, but most often at temperature below 25 °C. Therefore, the influence of the temperature is analyzed. It is shown that three effects determine the PV module's behavior. First, the encapsulant can buffer less stress at colder temperatures. Second, the overall PV module's stiffness increases caused by the increase of the encapsulants storage modulus. This leads to lower deflections at the same load at colder temperatures. Third, the third principal stress,

caused by thermal compression increases significantly when going to colder temperatures. The first effect is more dominant at higher temperatures and opposes the latter two effects, that are more dominant at lower temperatures. Therefore, a peak at a specific temperature where the probability of cell fracture is the highest can be seen.
Concluding, the inhomogeneous loading leads to a significant change in the solar cell's stress distribution, with a lower overall first principal stress as well as a lower probability of cell fracture. Here it is to mention that also the PV module's frame is loaded differently what may cause other failure pictures and is part of current and future work. Even though the cells are less prone to failure the inhomogeneous load test is a valuable addition to the homogeneous load described in the IEC 61215.

4 REFERENCES

[1] *Terrestrial photovoltaic (PV) modules – Design qualification and type approval – Part 1: Test requirements*, IEC 61215-1:2016, International Electrotechnical Commission (IEC), Geneva, Switzerland, 2016.

[2] *Photovoltaic (PV) modules - Non-uniform snow load testing*, IEC 62938:2020, International Electrotechnical Commission (IEC), May. 2020.

[3] S. Dietrich, "Numerische Untersuchungen zur mechanischen Zuverlässigkeit verkapselter Siliziumsolarzellen," Dissertation, Fakultät für Maschinenbau, Otto-von-Guericke-Universität Magdeburg, Halle (Saale), 2014.

[4] A. J. Beinert, P. Romer, M. Heinrich, M. Mittag, J. Aktaa, and H. Neuhaus, "The Effect of Cell and Module Dimensions on Thermomechanical Stress in PV Modules," *IEEE J. Photovoltaics*, vol. 10, no. 1, pp. 70–77, 2020, doi: 10.1109/JPHOTOV.2019.2949875.

[5] P. Romer, G. Oreski, A. J. Beinert, D. H. Neuhaus, and M. Mittag, "More Realistic Consideration of Backsheets Coefficient of Thermal Expansion on Thermomechanics of PV Modules," in *Proceedings of the 37th European Photovoltaic Solar Energy Conference and Exhibition (EU PVSEC)*, online, 2020, pp. 772–776.

[6] A. J. Beinert, P. Romer, M. Heinrich, M. Mittag, J. Aktaa, and H. Neuhaus, "Thermomechanical evaluation of new PV module designs by FEM simulations," in *Proceedings of the 36th European Photovoltaic Solar Energy Conference and Exhibition*, Marseille, France, 2019, pp. 783–788.

[7] A. J. Beinert, M. Ebert, U. Eitner, and J. Aktaa, "Influence of photovoltaic module mounting systems on the thermo-mechanical stresses in solar cells by FEM modelling," in *Proceedings of the 32nd European Photovoltaic Solar Energy Conference and Exhibition*, Munich, Germany, 2016, pp. 1833–1836.

[8] S. Dietrich, M. Sander, M. Pander, and M. Ebert, "Interdependency of mechanical failure rate of encapsulated solar cells and module design parameters," in *Proceedings of the SPIE Solar Energy + Technology*, San Diego, California, USA, 2012, 84720P-1-84720P-9.

[9] J. Y. Hartley *et al.*, "Effects of Photovoltaic Module Materials and Design on Module Deformation Under Load," *IEEE Journal of Photovoltaics*, vol. 10, no. 3, pp. 838–843, 2020, doi: 10.1109/JPHOTOV.2020.2971139.

[10] M. Aßmus, S. Bergmann, K. Naumenko, and H. Altenbach, "Mechanical behaviour of photovoltaic composite structures: A parameter study on the influence of geometric dimensions and material properties under static loading," *Composites Communications*, vol. 5, pp. 23–26, 2017, doi: 10.1016/j.coco.2017.06.003.

[11] S. Dietrich, U. Zeller, M. Pander, and M. Ebert, "Evaluation of non-uniform mechanical loads on solar modules," in.

[12] M. Aßmus, S. Bergmann, J. Eisenträger, K. Naumenko, and H. Altenbach, "Consideration of Non-uniform and Non-orthogonal Mechanical Loads for Structural Analysis of Photovoltaic Composite Structures," in *Advanced Structured Materials*, vol. 46, *Mechanics for materials and technologies*, H. Altenbach, R. V. Goldstein, and E. Murashkin, Eds., Basel, Switzerland: Springer International Publishing, 2017, pp. 73–122.

[13] A. M. Gabor, R. Janoch, A. Anselmo, J. L. Lincoln, H. Seigneur, and C. Honeker, "Mechanical load testing of solar panels — Beyond certification testing," in *2016 IEEE 43rd Photovoltaic Specialists Conference (PVSC)*, Portland, OR, USA, Jun. 2016 - Jun. 2016, pp. 3574–3579.

[14] G. Muelhoefer, H. Berg, C. Ferrara, W. Grzesik, and D. Philipp, "Influence of mechanical load at low temperatures on cell defects and power degradation in full-scale PV modules," in *Proceedings of the 28th European Photovoltaic Solar Energy Conference and Exhibition*, Paris, France, 2013, pp. 2968–2971.

[15] R. B. Roberts, "Thermal expansion reference data: silicon 300-850 K," *Journal of Physics D: Applied Physics*, vol. 14, no. 10, L163-163, 1981.

[16] R. B. Roberts, "Thermal expansion reference data: silicon 80-280K," *Journal of Physics D: Applied Physics*, vol. 15, no. 9, L119-120, 1982.

[17] U. Eitner, S. Kajari-Schroeder, M. Koentges, and H. Altenbach, "Thermal stress and strain of solar cells in photovoltaic modules," in *Advanced Structured Materials*, vol. 15, *Shell-like Structures: Non-classical Theories and Applications*, H. Altenbach and V. A. Eremeyev, Eds., Berlin/Heidelberg: Springer, 2011.

[18] W. M. Haynes, Ed., *CRC handbook of chemistry and physics*: CRC Press, 2014.

[19] W. Weibull, *A Statistical Theory of the Strength of Materials*. Stockholm: Generalstabens Litografiska Anstalts Förlag, 1939.

[20] D. Munz and T. Fett, *Ceramics: Mechanical properties, failure behaviour, materials selection*, 1st ed. Berlin | Heidelberg: Springer, 2001.

[21] F. Kaule, M. Pander, M. Turek, M. Grimm, E. Hofmueller, and S. Schoenfelder, "Mechanical damage of half-cell cutting technologies in solar cells and module laminates," in *SiliconPV 2018, The 8th International Conference on Crystalline Silicon Photovoltaics: Conference date, 19-21 March 2018 : location, Lausanne, Switzerland*, 2018, p. 20013.